

Observation of a Transition from BCS to HTSC-like Superconductivity in $\text{Ba}_{1-x}\text{K}_x\text{BiO}_3$ Single Crystals

G. É. Tsydynzhapov*, A. F. Shevchun, M. R. Trunin, V. N. Zverev, D. V. Shovkun, N. V. Barkovskiy, and L. A. Klinkova

Institute of Solid State Physics, Russian Academy of Sciences, Chernogolovka, Moscow region, 142432 Russia

* e-mail: gombo@issp.ac.ru

Received March 31, 2006

The temperature dependences of the upper critical field $B_{c2}(T)$ and surface impedance $Z(T) = R(T) + iX(T)$ have been measured in $\text{Ba}_{1-x}\text{K}_x\text{BiO}_3$ single crystals with transition temperatures $6 \leq T_c \leq 32$ K ($0.6 > x > 0.4$). A transition from the BCS to an unusual type of superconductivity has been revealed: $B_{c2}(T)$ curves of the crystals with $T_c > 20$ K have positive curvature (as in some HTSCs), and those of the crystals with $T_c < 15$ K described by the usual Werthamer–Helfand–Hohenberg (WHH) formula. The $R(T)$ and $X(T)$ dependences of the crystals with $T_c \approx 32$ K and $T_c \approx 11$ K in the temperature range $T \ll T_c$ are linear (as in HTSCs) and exponential (BCS), respectively. The experimental results are discussed using the extended saddle point model by Abrikosov.

PACS numbers: 74.20.-z, 74.70.-b

DOI: 10.1134/S0021364006090086

The $\text{Ba}_{1-x}\text{K}_x\text{BiO}_3$ compound undergoes a series of phase transformations on potassium doping. The base composition BaBiO_3 should be a metal with half-filled conduction band according to the band structure calculations [1]. However, it is an insulator due to the formation of a charge density wave, which distorts its perovskite lattice to monoclinic. The insulating state exists up to $x \approx 0.4$, while the monoclinic symmetry is replaced by the orthorhombic one at $x \approx 0.13$. At the transition into the metallic phase ($x > 0.4$), the lattice becomes cubic and no structural transitions are observed with the further increase in x [2]. The deformations of the lattice are small and it remains quasi-cubic for all x values.

Metallic $\text{Ba}_{1-x}\text{K}_x\text{BiO}_3$ is a superconductor. The superconducting transition temperature of optimally doped $\text{Ba}_{1-x}\text{K}_x\text{BiO}_3$ ($x \approx 0.4$) is quite high ($T_c \approx 32$ K) and it is usually considered to be an HTSC. However, $\text{Ba}_{1-x}\text{K}_x\text{BiO}_3$ contains no transition metal atoms, has no counterparts for CuO_2 planes, and its properties are isotropic.

One of the striking features common for cuprate HTSCs and $\text{Ba}_{1-x}\text{K}_x\text{BiO}_3$ is the positive curvature of the upper critical field temperature dependence $B_{c2}(T)$ determined by transport measurements. In the case of optimally doped $\text{Ba}_{0.6}\text{K}_{0.4}\text{BiO}_3$, this behavior was observed in [3, 4]. As was noted in [5], the temperature dependence of $B_{c2}(T)$ plotted for $\text{Ba}_{0.6}\text{K}_{0.4}\text{BiO}_3$ in reduced scales coincides with that for $\text{Tl}_2\text{Ba}_2\text{CuO}_6$ [6] or $\text{Bi}_2\text{Sr}_2\text{CaCuO}_8$ [7]. It is well known that measurements of the upper critical field of HTSC using different methods produce inconsistent results; the same is true for $\text{Ba}_{0.6}\text{K}_{0.4}\text{BiO}_3$ [8, 9].

Another common property of cuprate HTSCs and $\text{Ba}_{1-x}\text{K}_x\text{BiO}_3$ is the linear temperature dependence of both components of the complex surface impedance $Z(T) = R(T) + iX(T)$ in $T < T_c/2$ range [10], which is typical for the d -wave symmetry of the order parameter. It is worth noting that results concerning the electromagnetic properties of $\text{Ba}_{1-x}\text{K}_x\text{BiO}_3$ are often contradictory, because it is difficult to prepare high-quality samples: even $\text{Ba}_{1-x}\text{K}_x\text{BiO}_3$ crystals grown under the same conditions frequently differ in composition and homogeneity.

In the present paper, we study the evolution of $B_{c2}(T)$ dependences for a series of $\text{Ba}_{1-x}\text{K}_x\text{BiO}_3$ crystals ($0.4 < x < 0.6$) with T_c values ranging from 32 to 5 K and find that, as x decreases (which corresponds to increasing T_c), a transition from BCS to HTSC-like superconductivity takes place. The conclusion is confirmed by measurements of the surface impedance $R(T)$ and $X(T)$ in the highest quality $\text{Ba}_{1-x}\text{K}_x\text{BiO}_3$ crystals with $T_c = 11$ and 32 K.

The production of high-quality single crystals of $\text{Ba}_{1-x}\text{K}_x\text{BiO}_3$ with the uniform distribution of potassium at different x values is a very difficult task. Our samples were grown by the electrochemical deposition method described in [11, 12]. The crystals were black with a blue-green shine and had a roughly cubic shape, well-defined faces, and volume ranging from 0.2 to 2 mm³. We tried to obtain a series of crystals with different potassium contents covering as wide a range of the superconducting transition temperature T_c as possible, provided that the uniformity of composition within every crystal is maintained. Since even crystals origi-

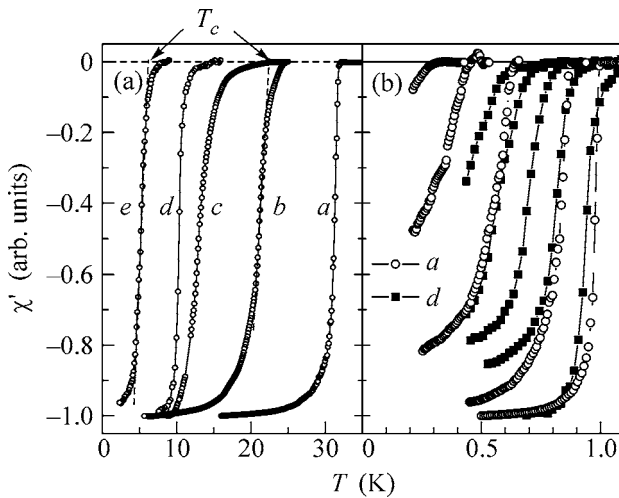


Fig. 1. (a) Superconducting transition curves obtained for $\text{Ba}_{1-x}\text{K}_x\text{BiO}_3$ crystals by measuring ac susceptibility $\chi'(T)$. The procedure used in this work to determine the transition point T_c is shown for samples *b* and *e*; (b) the effect of the magnetic field B on the $\chi'(T)$ curves of the crystals (circles) *a* and (squares) *d*. The field values (from right to left) $B = 0, 1, 6, 12,$ and 19.5 T for sample *a* and $B = 0, 0.067, 0.133, 0.2,$ and 0.27 T for sample *d*. Data for sample *a* are taken from [4].

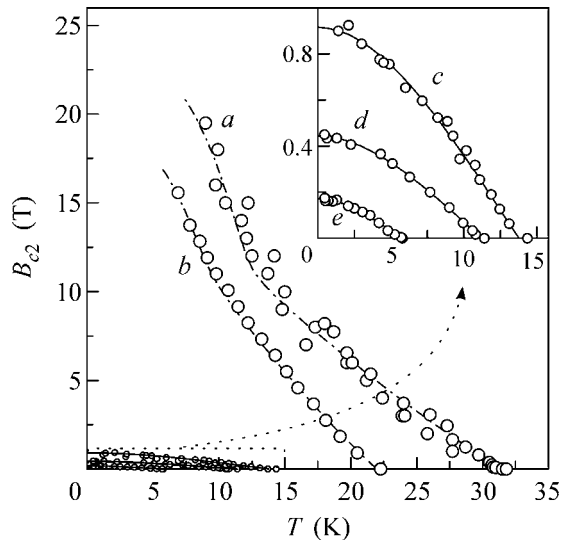


Fig. 2. Temperature dependences of the upper critical field for samples *a–e*. The dot-dashed lines present $B_{c2}(T)$ dependences calculated using the extended saddle point model [16]. The inset shows the left lower corner of the main plot in more detail. The solid lines are Werthamer–Helfand–Hohenberg (WHH) fits.

nating from one batch have significant variation in T_c (sometimes as large as 10 K), all samples were preliminary tested by measurements of the temperature dependences of ac susceptibility $\chi(T)$. Only samples with the narrowest and most regular superconducting transitions were selected for further experiments.

Measurement of ac susceptibility $\chi(T)$ in application to superconductors is similar to investigation of dc resistivity. In our case, the frequency of ac magnetic field excitation was 100 kHz and its amplitude was less than 0.1 Oe. A static external magnetic field up to 17 T was created by a superconducting magnet and was perpendicular to the ac field. Samples were not oriented in any special way with respect to the field, though we checked that results were reproduced for different positions of the crystals. The T_c point was determined from the transition curve as the intersection of the tangent that is drawn at the inflection point of the transition curve and the zero level that corresponds to the normal state (see Fig. 1a).

The temperature dependences of surface impedance $Z(T)$ were measured using the resonance technique described in [13] at $\omega/2\pi = 28.2$ GHz in a temperature range from 0.4 to 120 K. The H_{011} mode of a cylindrical niobium cavity was employed (the quality factor of the empty cavity was $\approx 2 \times 10^6$ in all operating temperature range); the amplitude of the microwave magnetic field on the sample surface was less than 1 Oe. The experimental setup and method of measurements were described in detail in [14].

The temperature dependences of the real part of the ac susceptibility $\chi'(T)$ for all samples with different potassium doping levels that are studied in this paper are shown in Fig. 1a. (The transition temperature decreases when x increases.)

Superconductivity is suppressed when magnetic field B is applied. This process is illustrated in Fig. 1b for samples *a* (the data for this sample are taken from our previous work [4]) and *d*. We emphasize that, in spite of the tremendous, more than ten times, difference between the field values $\chi'(T)$, the curves for these samples that correspond to the same reduced temperature T/T_c have about the same relative transition width and are generally similar to each other. This fact is important, because there is no rigorous, theoretically justified method to find the T_c point from a nonzero-width transition curve. It is possible that the widespread method we employ (Fig. 1a) introduces a systematic error. Figure 1 strongly suggests that this error, if any, is identical for different samples.

Figure 2 shows the $B_{c2}(T)$ curves for all samples studied. For crystals *c*, *d*, and *e* with $T_c = 14, 11,$ and 6 K, respectively, $B_{c2}(0)$ values do not exceed 1 T and the curvature of $B_{c2}(T)$ is negative. The temperature dependences of the upper critical field of these samples are in complete agreement with the Werthamer–Helfand–Hohenberg (WHH) formula derived in the BCS model. The estimations of the coherence length using the formula $B_{c2}(0) = \Phi_0/2\pi\xi(0)^2$ give 20, 30, and 40 nm for samples *c*, *d*, and *e*, respectively.

The $B_{c2}(T)$ curves for crystals *a* and *b* ($T_c = 32$ and 22 K, respectively) have positive curvature. The upper critical field at $T = 0$ is higher than that for crystals *c*, *d*,

and e by a factor of several tens, though available data are insufficient to make even a rough estimate of its value. At the very least, $B_{c2}(0)$ of sample a is higher than 25 T; correspondingly, $\xi(0)$ is no more than 4 nm. The dot-dashed lines in Fig. 2 are plotted according to the Abrikosov theory [15, 16]. The curves are obtained by numerically solving Eq. (15) from [16] using the following parameter values (for notation see [16]): $\eta = 1$ and $\alpha = 4\pi m_x T_c / \mu_1 m_e = 0.8$ for sample a ; and $\eta = 0.9$ and $\alpha = 1.2$ for sample b [17].

The $B_{c2}(T)$ curves shown in Fig. 2 demonstrate that the nature of superconductivity in $\text{Ba}_{1-x}\text{K}_x\text{BiO}_3$ changes as potassium doping increases: it turns from an unusual superconductivity to standard BCS superconductivity.

Microwave measurements confirm this conclusion. This technique reveals another important characteristic of superconducting sample quality in addition to the width of superconducting transition: it is the residual surface resistance $R_{\text{res}} = R(0)$. It is well known that the low-temperature features of the surface impedance $Z(T)$ in the imperfect crystals are masked by a high level of residual losses [13]. For this reason, they can be observed only in samples with the lowest R_{res} values. In this work, only sample d among the samples under investigation satisfies this selection criterion. The temperature dependences of the impedance components for this crystal are shown in Fig. 3. For $T > T_c$, the normal skin-effect condition $R(T) = X(T)$ is fulfilled. Therefore, the temperature dependence of the resistivity $\rho(T) = 2R^2(T)/\omega\mu_0$ can be derived; it is shown in the inset. The low-temperature parts of the $R(T)$ and $\lambda(T) = X(T)/\omega\mu_0$ curves are shown in Fig. 4. As in classical superconductors, the resistance $R(T)$ of sample d is saturated at the temperature-independent level of residual losses $R_{\text{res}} \approx 11.5 \text{ m}\Omega$ for $T < T_c/4$ and the field penetration depth reaches $\lambda(0) \approx 900 \text{ nm}$ at $T \rightarrow 0$. As shown in the inset of Fig. 4, both quantities exponentially approach saturation levels, in complete agreement with the BCS theory: $\Delta R(T) \propto (1/T)\exp(-\Delta_0/kT)$, $\Delta\lambda(T) \propto (1/\sqrt{T})\exp(-\Delta_0/kT)$, where Δ_0 is the superconducting gap at $T = 0$. The Δ_0 values derived from these curves agree well with each other and give $\Delta_0 \approx 2.1k_B T_c$, which means that the electron-phonon coupling constant in $\text{Ba}_{1-x}\text{K}_x\text{BiO}_3$ is not small. Using the well-known BCS equations, we obtain a number of sample parameters: the relaxation time $\tau \approx 6 \times 10^{-13} \text{ s}$ at $T = T_c$, average Fermi velocity $v_F \approx 3 \times 10^5 \text{ m/s}$ (which is about one third of the value following from the band structure calculations [1]), and carrier mean free path $l \approx 180 \text{ nm}$. According to these estimates, crystal d is a clean-limit London superconductor.

The surface impedance of the optimally doped $\text{Ba}_{0.6}\text{K}_{0.4}\text{BiO}_3$ crystal ($T_c \approx 30 \text{ K}$) was measured at 9.4 GHz in our previous work [10]. As in tetragonal HTSCs, we observed nearly linear temperature depen-

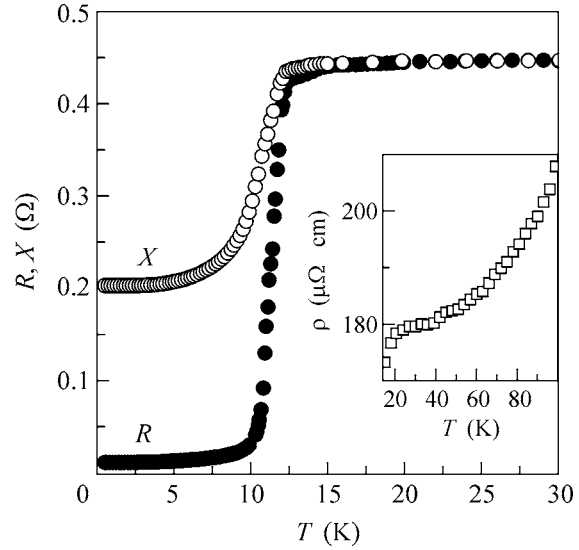


Fig. 3. Temperature dependences of the surface resistance $R(T)$ and reactance $X(T)$ in superconducting and (fragment) normal states of sample d at 28.2 GHz. The inset shows $\rho(T)$ dependence in $10 < T \leq 100 \text{ K}$ range.

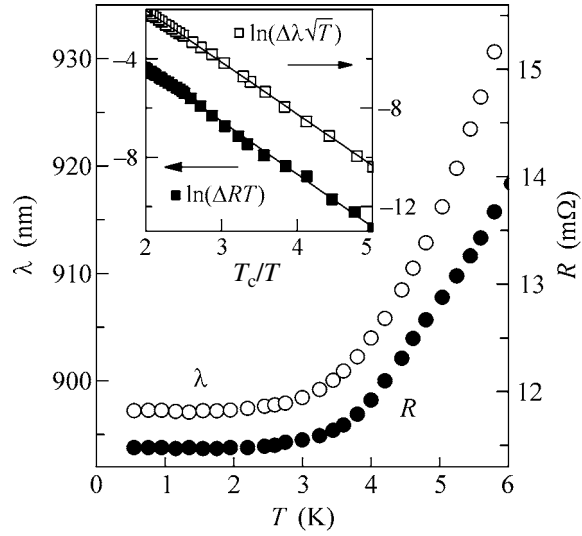


Fig. 4. Temperature dependences $R(T)$ and $\lambda(T) = X(T)/\omega\mu_0$ for sample d at low temperatures. The inset shows logarithms of (closed squares) $T\Delta R(T) = T[R(T) - R_{\text{res}}]$ and (open squares) $\sqrt{T}\Delta\lambda(T) = \sqrt{T}[\lambda(T) - \lambda(0)]$ in comparison to (solid lines) the predictions of the BCS model; their slopes give the gap value $\Delta(0)$.

dences of $\lambda(T)$ and $R(T)$ for $T < T_c/2$ [10, 13]; their extrapolations to $T \rightarrow 0$ give $\lambda(0) \approx 300 \text{ nm}$ and $R_{\text{res}} \approx 10 \text{ m}\Omega$. Hence, microwave measurements confirm that the natures of superconductivity of the samples with $T_c = 11 \text{ K}$ and the optimally doped samples are fundamentally different: the former are BCS-type superconductors, whereas the latter resemble cuprate HTSCs.

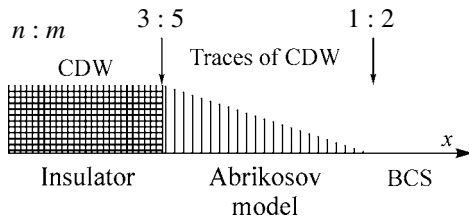


Fig. 5. Hypothetical phase diagram of $\text{Ba}_{1-x}\text{K}_x\text{BiO}_3$. The Ba-to-Bi content ratios $n : m$ that correspond to presumed phase boundaries are indicated.

The origin of the transition from HTSC-like to BCS superconductivity in the $\text{Ba}_{1-x}\text{K}_x\text{BiO}_3$ compound, which is revealed in this work, should be sought in the transformation of its crystal and electronic structure.

According to the hypothesis proposed in [11, 12], $\text{Ba}_{1-x}\text{K}_x\text{BiO}_3$ is formed from oxides of homologous series $\text{Ba}_n\text{Bi}_m\text{O}_y$ by means of potassium intercalation. The lattice of these oxides consists of alternating BiO_2 and BaO layers that form a supercell whose size depends on the ratio $n : m$. Potassium is intercalated into $\text{Ba}_n\text{Bi}_m\text{O}_y$ between adjacent BiO_2 layers (“bismuth planes”) and the $\text{Ba}_n\text{K}_{m-n}\text{Bi}_m\text{O}_{3m}$ composition is formed, where the number of Bi ions with an oxidation number of +5 in the bismuth planes next to potassium layers increases. As a result, x can assume only the values that correspond to a rational fraction $n : m$ of Ba and Bi content. As was shown in [18], the anisotropic $\text{Ba}_n\text{Bi}_m\text{O}_y$ matrix has a mosaic structure at the microscopic level; its lattice consists of ordered blocks that are displaced by a period of the quasi-cubic lattice. When the fraction $n : m$ decreases, the block size decreases and the layered structure completely disappears at $n : m = 1 : 2$. Applying these results to $\text{Ba}_{1-x}\text{K}_x\text{BiO}_3$, we find that a truly isotropic phase is formed at $x = 0.5$ ($n : m = 1 : 2$) rather than at $x = 0.4$ ($n : m = 3 : 5$). Local lattice anisotropy was observed in $\text{Ba}_{0.6}\text{K}_{0.4}\text{BiO}_3$ by electron microscopy [19]. It is not observed in the macroscopic properties, probably because of the mosaic lattice structure and easy twinning, i.e., because of absence of the long-range order in potassium positions.

The arrangement of potassium atoms into layers, together with the change in the oxidation number of Bi ions in the adjacent bismuth planes, leads to the modulation of the space charge. In the case with a long-range order (for $n/m \sim 1$), it signifies the formation of a charge density wave (CDW). It is the CDW that is responsible for the insulating state of $\text{Ba}_{1-x}\text{K}_x\text{BiO}_3$ for $x < 0.4$. As the size of lattice blocks of $\text{Ba}_n\text{Bi}_m\text{O}_y$ matrix decreases, the long-range order disappears, but charge is still ordered at the microscopic level (the short-range order) until the layered structure of the matrix is completely destroyed. According to this concept, a residual effect (“traces”) of the CDW should be retained in the metallic phase of $\text{Ba}_{1-x}\text{K}_x\text{BiO}_3$ in the potassium content

range from $x = 0.4$ to 0.5. Such traces were really observed in the Compton positron scattering [20] and IR conductivity [21] experiments. Since high-temperature superconductivity in $\text{Ba}_{1-x}\text{K}_x\text{BiO}_3$ is observed roughly in the same composition region, it is possible that the traces of the CDW play a crucial role in its origin.

A connection between the influence of the CDW and superconductivity may be established in the Abrikosov model [15]. According to it, many features of HTSC including high transition temperature, d -wave symmetry of the order parameter, and the positive curvature of $B_{c2}(T)$ can be explained if the electronic spectrum contains an extended saddle point (i.e., a flat piece of an equipotential surface) and the Fermi energy is close to it. Suitable conditions in $\text{Ba}_{1-x}\text{K}_x\text{BiO}_3$ can be formed because of the influence of the CDW. According to [20], the traces of CDW are manifested as a suppressed electron density of states near the middle of diagonal of the Brillouin zone (L point); it is exactly where the Fermi surface is located at $x = 0.4$ [1]. Assuming that suppression forms a flat part of the spectrum, we can apply the Abrikosov model to explain all our observations: (i) the linear temperature dependences of $\lambda(T)$ and $R(T)$ follow from d -wave symmetry of the order parameter and (ii) the upper critical field curves of samples a and b fit the theoretical dependences well (Fig. 2).

The Abrikosov model has a key advantage in respect to application to $\text{Ba}_{1-x}\text{K}_x\text{BiO}_3$: the dominating pairing mechanism both in the Abrikosov and BCS models is the electron–phonon interaction. Therefore, a transition from one model to another can occur naturally, as illustrated by the diagram in Fig. 5. At small x values, the long-range order in the positions of Bi^{5+} ions is maintained in the crystals; i.e., the charge density wave is present and opens a gap at the Fermi surface; thus, the compound is an insulator. At the transition to the superconducting metallic phase at $x = 0.4$ ($n : m = 3 : 5$), the long-range order disappears, but, presumably, a short-range order of bismuth ions with different oxidation numbers remains. It is manifested in various traces of the charge density wave, one of which can be flat parts of the spectrum formed due to the suppression of the density of states in the L points in the Brillouin zone. Within the Abrikosov model, the existence of such flat part of the spectrum leads to a high transition temperature, the d -wave symmetry of the order parameter [and, consequently, to the linear temperature dependences of $\lambda(T)$ and $R(T)$], and positive curvature of $B_{c2}(T)$. With a further increase in x , the short-range order is destroyed and simultaneously the Fermi surface contracts and moves away from the degenerate point of the Brillouin zone. Owing to one or both of these factors, the Abrikosov mechanism eventually breaks down, but the electron–phonon coupling makes sure that superconductivity remains, now in the BCS form. If the latter transition is caused by complete loss of the short-range order (dis-

appearance of any traces of the CDW), then it probably takes place at $n : m = 1 : 2$ ($x = 0.5$).

Thus, the $\text{Ba}_{1-x}\text{K}_x\text{BiO}_3$ compound is a unique object exhibiting a transition from HTSC to BCS superconductivity in the metallic phase ($x > 0.4$) when potassium doping x increases. We observe it clearly in measurements of the temperature dependences of the upper critical field $B_{c2}(T)$ and surface impedance $Z(T)$ of a series of $\text{Ba}_{1-x}\text{K}_x\text{BiO}_3$ single crystals. The change in the nature of superconductivity can be due to the special features of the electron spectrum of $\text{Ba}_{1-x}\text{K}_x\text{BiO}_3$ that are associated with the residual effect of the charge density wave and the inclusion of the high-temperature superconductivity mechanism suggested by Abrikosov [15].

We are grateful to V.F. Gantmakher, A.A. Golubov, and V.I. Nikolaychik for their interest and helpful discussions. This work is supported by the Russian Foundation for Basic Research (project nos. 04-02-17358, 06-02-17098) and the Russian Academy of Sciences. G.E.Ts. acknowledges the support of the Council of the President of the Russian Federation for Support of Young Scientists and Leading Scientific Schools (project no. MK-4074.2005.2).

REFERENCES

1. S. Sahrakorpi, B. Barbiellini, R. S. Markiewicz, et al., Phys. Rev. B **61**, 7388 (2000).
2. S. Pei, J. D. Jorgensen, B. Dabrowski, et al., Phys. Rev. B **49**, 4126 (1990).
3. M. Affronte, J. Marcus, C. Escribe-Filippine, et al., Phys. Rev. B **49**, 3502 (1994).
4. V. F. Gantmakher, L. A. Klinkova, N. V. Barkovskii, et al., Phys. Rev. B **54**, 6133 (1996).
5. G. É. Tsydynzhapov, Candidate's Dissertation in Physics and Mathematics (Inst. of Solid State Physics, Russian Academy of Sciences, Chernogolovka, 1999).
6. A. P. Mackenzie, S. R. Julian, G. G. Lonzarich, et al., Phys. Rev. Lett. **71**, 1238 (1993).
7. M. S. Osofsky, R. J. Soulen, Jr., S. A. Wolf, et al., Phys. Rev. Lett. **71**, 2315 (1993).
8. P. Szabo, P. Samuely, T. Klein, et al., Europhys. Lett. **41**, 207 (1998).
9. S. Blanchard, T. Klein, J. Marcus, et al., Phys. Rev. Lett. **88**, 177201 (2002).
10. M. R. Trunin, A. A. Zhukov, and G. É. Tsydynzhapov, Pis'ma Zh. Éksp. Teor. Fiz. **64**, 783 (1996) [JETP Lett. **64**, 832 (1996)].
11. L. A. Klinkova, Sverkhprovodimost: Fiz. Khim. Tekh. **7**, 418 (1994).
12. L. A. Klinkova, V. I. Nikolaichik, N. V. Barkovskii, et al., Zh. Neorg. Khim. **46**, 715 (2001).
13. M. R. Trunin, Usp. Fiz. Nauk **168**, 931 (1998) [Phys. Usp. **41**, 843 (1998)]; Usp. Fiz. Nauk **175**, 1017 (2005) [Phys. Usp. **48**, 979 (2005)].
14. A. F. Shevchun and M. R. Trunin, Prib. Tekh. Éksp. (in press).
15. A. A. Abrikosov, Int. J. Mod. Phys. **13**, 3405 (1999).
16. A. A. Abrikosov, Phys. Rev. B **56**, 5112 (1997).
17. We believe that, owing to the features of the model, this equation can also be applied for qualitative comparison for $\text{Ba}_{1-x}\text{K}_x\text{BiO}_3$, although a strongly anisotropic material was considered in [16].
18. V. I. Nikolaichik, S. Amelinckx, L. A. Klinkova, et al., J. Solid State Chem. **163**, 44 (2002).
19. L. A. Klinkova, M. Uchida, Y. Matsui, et al., Phys. Rev. B **67**, R140501 (2003).
20. N. Hiraoka, T. Buslaps, V. Homkimaki, et al., Phys. Rev. B **71**, 205106 (2005).
21. S. H. Blanton, R. T. Collins, K. H. Kelleher, et al., Phys. Rev. B **47**, 996 (1993).

Translated by G. Tsydynzhapov